

Fission-Excitation Functions in Interactions of C^{12} , O^{16} , and Ne^{22} With Various Targets

TORBJØRN SIKKELAND

Lawrence Radiation Laboratory, University of California, Berkeley, California

(Received 26 March 1964)

The fission cross sections σ_f in the bombardment of Cs, Pr, Tb, Ho, Er¹⁷⁰, Tm, Yb¹⁷⁴, Lu, W¹⁸², Au, and Bi with O¹⁶, Tm with C¹², and Tb with Ne²² have been measured as a function of projectile energy. The technique consists of counting coincident fission-fragment pairs with two Au surface-barrier Si detectors. The results are given in units of the total interaction cross section σ_R , and as a function of the excitation energy E of the compound nucleus. It is demonstrated that for a constant value of E for a compound nucleus σ_f/σ_R is a function of the mass of the ion used and thus of the angular momentum of the nucleus. Fission for the systems investigated takes place only for nuclei formed in a complete fusion of the ion and the target nuclei. The cross section of σ_{CF} for this process is shown to be nearly independent of E and the target used. We find σ_{CF}/σ_R to be 0.70 and 0.45 for O¹⁶ and Ne²², respectively. From the ratio σ_f/σ_{CF} , experimental Γ_f/Γ_n values are obtained and compared to theoretical ones. The following values in MeV with a standard deviation of 2 MeV for the experimental fission threshold for a nonrotating nucleus are obtained: 34.9, 26.5, 25.1, 24.6, 24.2, 20.4, 19.8, 18.2, and 17.0 for the compound nuclei Eu¹⁴⁹, Ho¹⁵⁷, Ta¹⁷⁵, Re¹⁸¹, Os¹⁸⁶, Ir¹⁸⁶, Pt¹⁹⁰, Au¹⁹¹, and Po¹⁹⁸, respectively. These values, when corrected for shell effects, fit well the formula for a nonrotating charged liquid drop: $E_f^L = 6.76(0.75 - x)A^{2/3}$. Here, $x = (Z^2/A)/(Z^2/A)_{crit}$, and we obtain the value 48.0 ± 1.0 for $(Z^2/A)_{crit}$. The ratio between the level-density parameters for fission and neutron evaporation a_f/a_n is found to be 1.22 ± 0.05 ; this ratio is independent of nuclear type. In particular, the ratio is nearly the same inside and outside the region of the closed shell. Values for moments of inertia can not be evaluated from the analysis.

I. INTRODUCTION

FISSION cross sections induced by He⁴ have been measured for heavy elements ($Z > 90$, see Ref. 1) and for Au, Tl, Pb²⁰⁶, and Bi (Ref. 2). Similar measurements involving heavy ions of various energies have been performed for B¹¹, C¹², N¹⁴, O¹⁶, and Ne²⁰ incident on U²³⁸ (Ref. 3); N¹⁴ on Re, Au, and Bi (Ref. 4); C¹² and O¹⁶ on Au and Bi (Ref. 5); and C¹² on Tm and Re¹⁸⁵, O¹⁶ on Ho, Tm, Ta¹⁸¹ and Re¹⁸⁵, and Ne²⁰ on Ho and Ta¹⁸¹ (Ref. 6). Additionally, σ_f has been determined for C¹², O¹⁶, and Ne²⁰ of 10.4 MeV/nucleon interacting with both Pb²⁰⁸ and with Bi (Ref. 7).

A knowledge of fission-excitation functions is important for a proper investigation and interpretation of fragment angular distribution functions and of fragment kinetic energies. The quantity σ_f is then, given in units of the compound-nucleus cross section σ_C as a function of its excitation energy. At the steep part of the curve

for σ_f/σ_C , first chance fission is dominating and the fissioning nucleus and its excitation energy are known. By analyzing this region of the function it is possible to obtain values for the fission barrier. Such analysis has been performed for the heaviest nuclei,¹ and for nuclei in the closed-shell region around Pb²⁰⁸ (Ref. 2). It was then hoped to extend this analysis to lighter nuclei (outside the closed shell) that can be induced to undergo fission by heavy ions. A more direct comparison with liquid-drop-model calculations can then be made. Also, by the use of heavy ions, the influence of rotation on σ_f/σ_C and thus on the level widths for neutron evaporation and fission can be enhanced and studied.

In our work, the natural isotopes of Cs, Pr, Tb, Ho, Tm, and Lu, Au, and Bi, and Er¹⁷⁰, Yb¹⁷⁴, and W¹⁸², were bombarded with O¹⁶ of varying energies.

To study the effect of angular momentum l on the ratio σ_f/σ_C , we formed the same compound nucleus Re¹⁸¹ three ways: C¹²+Tm¹⁶⁹, O¹⁶+Ho¹⁶⁵, and Ne²²+Tb¹⁵⁹, having the same E but different l . A similar study of the angular-momentum effect has been undertaken by Gilmore⁶ using a technique where the fragments were caught in photographic emulsion. This method is probably not adequate in separating real fission-fragment tracks from other short-range reaction products. At the start of our investigation we intended to count fragments by analyzing the pulse-height spectrum obtained with one detector. Such single-spectrum analysis was found to be adequate in fission studies of Au and heavier targets.^{3,5} With lighter targets, however, the energies of the fragments are lower, making it impossible to separate the fission-fragment events from other reaction products. Instead, we had to use two detectors in connection with a coincident circuitry. This

* This work was performed under the auspices of the U. S. Atomic Energy Commission.

¹ Reference to some of these data can be found in a recent review article on fission by J. R. Huizenga and R. Vandenbosch, in *Nuclear Reactions*, edited by P. M. Endt and P. B. Smith (North-Holland Publishing Company, Amsterdam, 1962).

² J. R. Huizenga, R. Chaudhry, and R. Vandenbosch, *Phys. Rev.* **126**, 210 (1962).

³ V. E. Viola, Jr., and T. Sikkeland, *Phys. Rev.* **128**, 767 (1962).

⁴ S. M. Polikanov and V. A. Druin, *Zh. Eksperim. i Teor. Fiz.* **36**, 744 (1959) [English transl.: *Soviet Phys.—JETP* **9**, 522 (1959)].

⁵ H. C. Britt and A. R. Quinton, in *Proceedings of the Second Conference on Reactions Between Complex Nuclei, Gatlinburg, May 1960* (John Wiley & Sons, Inc., New York, 1960).

⁶ J. Gilmore, thesis, Lawrence Radiation Laboratory Report UCRL-9304, July 1960 (unpublished).

⁷ E. Goldberg, H. L. Reynolds, and D. D. Kerlee, in *Proceedings of the Second Conference on Reactions Between Complex Nuclei, Gatlinburg, May 1960* (John Wiley & Sons, Inc., New York, 1960).

TABLE I. Experimental fission cross section and the ratio

E_L	Cs+O ¹⁶		Pr+O ¹⁶		Tb+O ¹⁶		Ho+O ¹⁶		Er ¹⁷⁰ +O ¹⁶		Tm+O ¹⁶		Yb ¹⁷⁴ +O ¹⁶	
	σ_f (mb)	σ_f/σ_R	σ_f (mb)	σ_f/σ_R	σ_f (mb)	σ_f/σ_R	σ_f (mb)	σ_f/σ_R	σ_f (mb)	σ_f/σ_R	σ_f (mb)	σ_f/σ_R	σ_f (mb)	σ_f/σ_R
166.1	70.0	3.1×10^{-2}	130	5.8×10^{-2}	301	0.133	530	0.239	574	0.253	774	0.353	779	0.346
162.6	64.8	2.9×10^{-2}			279	0.125								
158.4	54.2	2.5×10^{-2}	107	4.9×10^{-2}	270	0.123	527	0.243	501	0.228	766	0.358		
154.9					245	0.114	442	0.206					750	0.350
151.9	31.7	1.5×10^{-2}	99.1	4.7×10^{-2}			412	0.195	494	0.228	626	0.300		
147.5					216	0.104	377	0.181						
143.2	22.5	1.1×10^{-2}	73.5	3.6×10^{-2}			377	0.185	395	0.193	625	0.312	579	0.289
139.2					174	8.9×10^{-2}	339	0.173						
135.7	13.6	6.8×10^{-3}	43.8	2.2×10^{-2}			299	0.156	298	0.155	498	0.262		
131.2			33.5	1.7×10^{-2}	118	6.3×10^{-2}	263	0.141			531	0.290	477	0.261
126.7	5.08	2.7×10^{-3}	24.7	1.3×10^{-2}	90	5.0×10^{-2}	199	0.111	206	0.114	387	0.221		
122.2	3.36	1.8×10^{-3}	14.4	8.1×10^{-3}	61	3.7×10^{-2}	171	0.101	150	8.7×10^{-2}				
118.2	1.38	7.8×10^{-4}	7.7	4.5×10^{-3}	44.	2.7×10^{-2}			118	7.2×10^{-2}	267	0.167	290	0.181
113.6	0.76	4.5×10^{-4}	3.7	2.3×10^{-3}	26.5	1.7×10^{-2}	61	4.0×10^{-2}	67	4.4×10^{-2}	186	0.124		
108.5			1.38	9.0×10^{-4}	14.9	1.0×10^{-2}	35	2.5×10^{-2}	36	2.5×10^{-2}	125	9.05×10^{-2}	128	9.3×10^{-2}
105.5					8.2	5.8×10^{-3}								
103.7					4.6	3.2×10^{-3}	20	1.5×10^{-2}	20	1.5×10^{-2}	67	5.4×10^{-2}	80	6.4×10^{-2}
101.0					3.7	2.9×10^{-3}								
99.0					2.5	2.0×10^{-3}	5.9	5.0×10^{-3}	5.9	5.0×10^{-3}	26	2.3×10^{-2}	35	3.1×10^{-2}
95.5					0.82	7.3×10^{-4}			2.4	2.2×10^{-3}				
93.4					0.61	5.7×10^{-4}	1.6	1.6×10^{-3}	1.8	1.8×10^{-3}	10.8	1.14×10^{-2}	13.2	1.40×10^{-2}
89.6														
87.7											3.2	4.2×10^{-3}	4.2	5.7×10^{-3}
84.3														
81.9													0.72	1.44×10^{-3}
77.8														

method should be superior to any other used so far since a fission event then is not only identified by the energy of the fragment but also by a coincident requirement. We therefore felt the work to be of importance from an experimental point of view.

II. EXPERIMENTAL PROCEDURE

Heavy-ion beams were obtained from the Berkeley HILAC, which accelerates ions to 10.4 MeV/nucleon. The beam was deflected through 30 deg by a magnet before reaching the fission and scatter chamber, which has been described in a previous paper.⁸ We obtained lower energies by inserting weighed aluminum foils into the beam path. Northcliffe's range-energy curves for aluminum were used to estimate the resulting energy.⁹ Additionally, the ranges of the ions in emulsion were measured; from this the average energy and the energy spread could be evaluated.¹⁰ The average energies obtained with the two methods were generally in agreement at the highest energies, but differed as much as 2 MeV at the lowest energies.

Before striking the target, the beam passed through two circular collimators 1.5 mm in diameter and 62 cm apart. The last collimator was 6 cm from the target. Beam particles were collected in a 7.5-cm-wide Faraday cup at the rear of the chamber and the current was measured with an electrometer, the output of which was fed to an integrator.

Targets were made by vaporizing the material onto 100- $\mu\text{g}/\text{cm}^2$ -thick nickel films. Target thicknesses were around 200 $\mu\text{g}/\text{cm}^2$. The quantity σ_f can be obtained by measuring with the same detector geometry and target

the relative differential cross section both for fission, $\xi_f(\psi)$, and for elastically scattered ions, $\xi_s(\psi)$. After proper transformation to the center-of-mass systems of the fissioning nucleus and of scatter, we obtain for binary fission

$$\sigma_f = \frac{\pi b^2 \xi_f(\pi/2)}{16 \xi_s(\theta_s) \sin^4(\theta_s/2)} \int \frac{\xi_f(\theta_f) \sin \theta_f d\theta_f}{\xi_f(\pi/2)}. \quad (1)$$

Here we have $b = Z_I Z_T e^2 (m_I + m_T) / (E_L m_T)$, where Z_I , m_I , and E_L are the atomic number, mass, and laboratory energy of the ion, and Z_T and m_T are the atomic number and mass of the target nucleus, while θ_s and θ_f are the angles in the c.m. of the scatter and of the fissioning nucleus, respectively. The transformation is accomplished with the parameter $x^2 = (V/v)^2$, where V is the velocity of the center of mass and v the velocity of the reaction product in the c.m. In elastic scattering, we have $x^2 = (m_I/m_T)^2$. For fission the most probable value x_{mp}^2 is obtained from fragment-fragment angular-correlation-function measurements as described in an earlier paper.⁸ At the peak for this function we have

$$\tan \psi_1 = (\sin \theta) / (x_{mp} + \cos \theta) \quad (2)$$

and

$$\tan \psi_2 = (\sin \theta) / (x_{mp} - \cos \theta), \quad (3)$$

where ψ_1 and ψ_2 are the laboratory angles between the beam axis and the axis of the two detectors $D1$ and $D2$. In previous works,^{3,11} σ_f was determined according to Eq. (1) by the use of one detector.^{3,11} With U^{238} and ions up to Ne^{20} , and with Au, Bi, and ions up to O^{16} , a satisfactory separation of the fission-fragment pulses and pulses from other reaction products is possible. However, with heavy ions incident on lighter targets and ions heavier than O^{16} incident on Au and Bi, this

⁸ T. Sikkeland, E. L. Haines, and V. E. Viola, Jr., Phys. Rev. 125, 1350 (1960).

⁹ L. C. Northcliffe, Phys. Rev. 120, 1744 (1960).

¹⁰ P. G. Roll and F. E. Steigert, Yale University (private communication).

¹¹ T. Sikkeland, A. E. Larsh, and G. E. Gordon, Phys. Rev. 123, 2112 (1961).

σ_f/σ_R at various ion energies for systems investigated.

Lu + O ¹⁶		W ¹⁸² + O ¹⁶		Au + O ¹⁶		Bi + O ¹⁶		Tm + C ¹²			Tb + Ne ²²		
σ_f (mb)	σ_f/σ_R	σ_f (mb)	σ_f/σ_R	σ_f (mb)	σ_f/σ_R	σ_f (mb)	σ_f/σ_R	E_L	σ_f (mb)	σ_f/σ_R	E_L	σ_f (mb)	σ_f/σ_R
1242	0.558	1507	0.701	1556	0.717	1500	0.688	124.6	147	6.89×10^{-2}	228.4	1139	0.46
1187	0.557	1344	0.640	1500	0.714	1456	0.707	122.4	129	6.06×10^{-2}	223.3	1118	0.46
1138	0.547	1362	0.673	1400	0.694	1420	0.719	120.2	104	5.00×10^{-2}	218.2	1091	0.45
1082	0.549	1224	0.631	1384	0.744	1320	0.71	116.3	93.5	4.50×10^{-2}	211.2	1147	0.48
901	0.484	1197	0.656	1267	0.708	1190	0.66	114.2	83.9	4.17×10^{-2}	205.9	1026	0.44
741	0.432	1044	0.621	1141	0.702	1180	0.68	111.8	64.1	3.23×10^{-2}	200.0	1020	0.44
557	0.357	905	0.600	956	0.671	1170	0.86	107.8	41.9	2.18×10^{-2}	193.4	974	0.44
461	0.316					1180	0.68	105.4	37.2	1.98×10^{-2}	187.0	984	0.45
317	0.236	689	0.541	800	0.681	1090	0.66	102.8	27.6	1.50×10^{-2}	181.5	950	0.45
233	0.191					990	0.68	100.6	23.5	1.31×10^{-2}	174.7	911	0.44
104	9.7×10^{-2}	371	0.37	475	0.54	900	0.68	98.2	14.9	8.5×10^{-3}	167.6	779	0.40
62	6.4×10^{-2}					1170	0.86	95.8	14.8	8.8×10^{-3}	162.8	725	0.38
39	4.3×10^{-2}	186	0.23	333	0.49	840	0.68	93.2	9.2	5.7×10^{-3}	154.4	646	0.36
24	3.1×10^{-2}	102	0.16	213	0.41	840	0.68	90.6	6.4	4.1×10^{-3}	147.4	493	0.29
13.6	2.0×10^{-2}	68	0.12	141	0.32	807	0.74	88.1	3.9	2.6×10^{-3}	139.5	383	0.24
3.6	6.5×10^{-3}	23	5.4×10^{-2}	65	0.24			85.6	2.3	1.6×10^{-3}	132.0	233	0.16
1.31	2.9×10^{-3}	3.0	1.9×10^{-2}					82.7	1.9	1.4×10^{-3}	124.1	93.5	7.5×10^{-2}
				0.32	2.5×10^{-2}			79.8	1.0	8.1×10^{-4}	118.4	33.2	3.0×10^{-2}
								77.9	0.65	5.4×10^{-4}	115.9	20.4	1.9×10^{-2}
								74.3	0.19	1.7×10^{-4}	110.9	7.2	7.7×10^{-3}
											101.0	1.0	1.7×10^{-3}

separation was impossible. Instead, we had to perform the counting of the fragments with two detectors by using a standard fast-slow coincidence technique. The electronic system and scattering chamber used have been described in earlier publications.^{7,12}

In the fission-differential cross-section measurements, the two detectors were placed at the angles ψ_1 and ψ_2 as determined from fragment-fragment correlation experiments. Detector $D1$ defined the geometry and was later used for measurements of $\xi_s(\psi)$. The geometry of $D2$ had to be large enough to catch practically all fragments in coincidence with the fragments entering $D1$. We used circular collimators for both detectors. The $D1$ collimator had a geometry of 1.4×10^{-3} sr, while that of $D2$ was 0.28 sr. The counting efficiency of this arrangement was checked for the system Au + 124-MeV C¹², where good single spectra could be obtained. We found $\xi_f(\psi)$ obtained from coincidence counting to be of the order of 95% of the value obtained from single-detector counting.

Fragment angular distributions could not be obtained with the coincidence technique since the geometry of $D2$ was too large to permit $\xi_f(\psi)$ to be measured at extreme forward or backward angles. Approximate distributions measured with a single detector indicated that for targets lighter than Au the distribution followed the $1/\sin\theta$ law up to 170 deg. For such a distribution, the value of the integral in Eq. (1) is π . It is expected that the actual distribution will be below that predicted by $1/\sin\theta$ at extreme angles. For the system U²³⁸ + C¹² the value of the integral decreases linearly with the C¹² energy from 0.90π at 124 MeV to 0.70π at 74-MeV C¹² (Ref. 11). The same value is around 0.95π for C¹², O¹⁶, and Ne²⁰ of 10.4 MeV/nucleon incident on Au and

0.88π for the system Bi + 166-MeV O¹⁶ (Ref. 13). For targets lighter than Au we have assumed the integral to have a value 0.95π at 10.4 MeV/nucleon decreasing linearly with ion energy to 0.85π at 6 MeV/nucleon. Errors introduced by this assumption are believed to be around 5%. (By errors here and later are meant standard deviation.)

III. EXPERIMENTAL RESULTS

Fission cross sections measured at various projectile energies for the different systems are given in Table I. In the same table we list the ratio σ_f/σ_R , where we

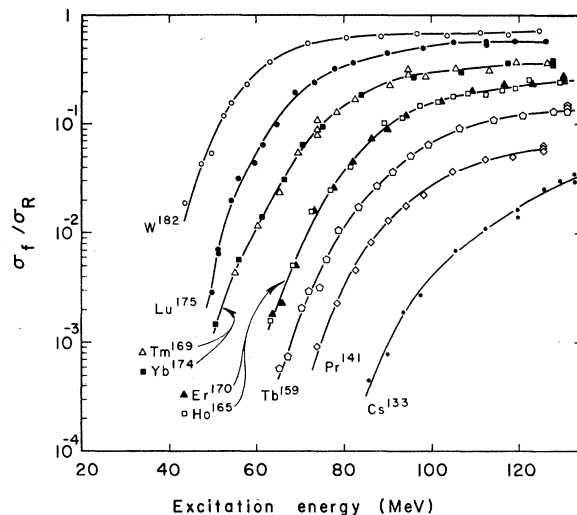


FIG. 1. Experimental values for the ratio σ_f/σ_R as function of the excitation energy in the bombardment of various targets with O¹⁶.

¹² T. Sikkeland and V. E. Viola, Jr., in *Proceedings of the Third Conference on Reactions Between Complex Nuclei, Asilomar, April 1963* (University of California Press, Berkeley, 1963).

¹³ Data obtained from author's fragment angular-distribution measurements.

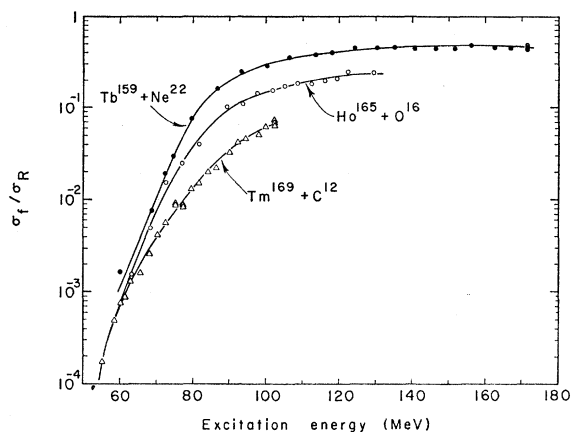


FIG. 2. Experimental values for the ratio σ_f/σ_R as function of the excitation energy for the compound nucleus Re^{181} formed in the reactions $\text{Tm} + \text{C}^{12}$, $\text{Ho} + \text{O}^{16}$, and $\text{Tb} + \text{Ne}^{22}$.

calculate σ_R , the total interaction cross section, by using a parabolic approximation to the optical-model real potential. The parameters used were taken from Viola and Sikkeland.³ It has been shown that these values reproduce total cross sections with U^{238} as the target if it is assumed that $\sigma_f = \sigma_R$. Wilkins and Igo have shown that the values are also applicable for lighter targets such as Al and Ag (Ref. 14). The ratio σ_f/σ_R is plotted versus E in Figs. 1 and 2, where E is the excitation energy of the compound nucleus formed in a complete fusion of ion and target nuclei as computed from E_L and the masses involved. The masses were taken from the compilation by Cameron.¹⁵ Generally, the errors were about 7% and include, according to

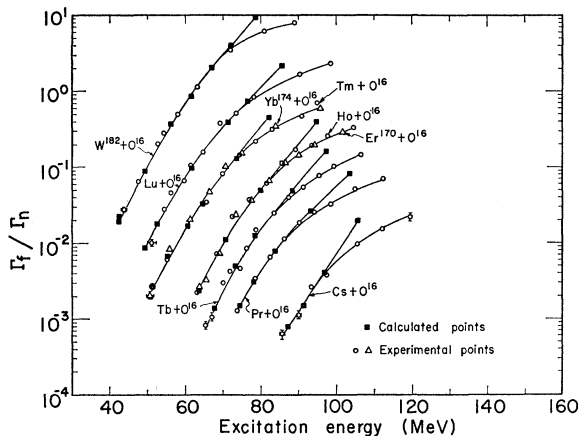


FIG. 3. Calculated and experimental Γ_f/Γ_n functions for nuclei formed in the bombardments of various targets with O^{16} : ■ calculated values; ○ △ experimental values.

¹⁴ B. Wilkins and G. Igo, in *Proceedings of the Third Conference on Reactions Between Complex Nuclei, Asilomar, April 1963* (University of California Press, Berkeley, 1963).

¹⁵ A. G. W. Cameron, Atomic Energy of Canada, Ltd., Report No. CRP-690, 1957 (unpublished).

formula (1), statistical errors in the counting, errors in the value of the integral, in the angles ψ_f and ψ_s . Typical values for the highest errors are given in Figs. 3 and 4.

The systems $\text{Bi} + \text{O}^{16}$ and $\text{Au} + \text{O}^{16}$ yield σ_f/σ_R values that are nearly constant for all values of E . The very steep part of σ_f at lowest E therefore reflects the influence of the Coulomb barrier on the reaction cross section. In this region, σ_f/σ_R will have large errors. Therefore, we have not plotted the σ_f/σ_R functions for these systems. The data for these two systems are in good agreement with those reported by Britt and Quinton.⁵ The fission cross-section data obtained for $\text{Tm} + \text{O}^{16}$ and $\text{Ho} + \text{O}^{16}$ agree well with those of Gilmore⁶ at the highest E values. At lower energies, his values

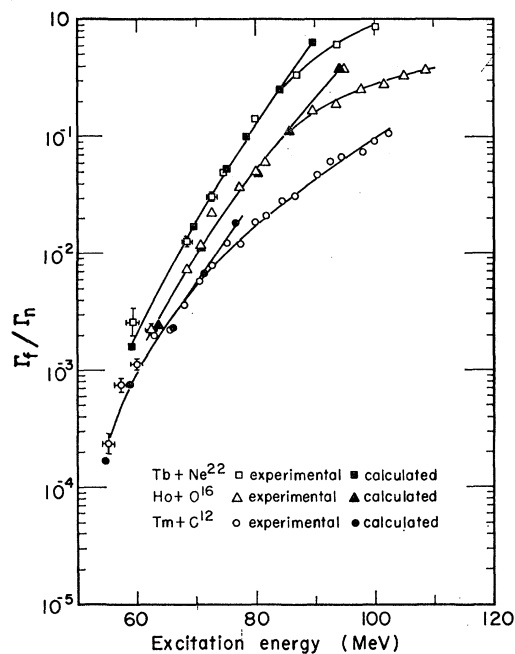


FIG. 4. Calculated and experimental Γ_f/Γ_n functions for the compound nucleus Re^{181} formed three ways. $\text{Tb} + \text{Ne}^{22}$: □ experimental, ■ calculated; $\text{Ho} + \text{O}^{16}$: △ experimental, ▲ calculated; $\text{Tm} + \text{C}^{12}$: ○ experimental, ● calculated.

are substantially higher than ours. We believe this is due to introduction of nonfission tracks in an emulsion.

IV. DISCUSSION

A. Evaluation of Experimental Γ_f/Γ_n Values

Fission at a measurable rate occurs from nuclei having excitation energies higher than the fission threshold. Such nuclei can be formed in nuclear reactions induced by heavy ions. We will divide these reactions into two groups. In the first group the ion and target nucleus are amalgamated in a complete fusion (CF) process. For this reaction, the compound nucleus and its excitation energy are known.

The second group consists of reactions in which

nucleons are interchanged between ion and target and an incomplete fusion (ICF) reaction takes place. Here the resulting compound nuclei have a whole spectrum of masses and excitation energies.

The reaction cross sections for the CF and the ICF processes will be denoted σ_{CF} and σ_{ICF} , respectively, and we have $\sigma_{CF} + \sigma_{ICF} = \sigma_R$. The compound nuclei formed in either processes may decay by fission or by evaporation of particles. If the excitation energy is high enough, fission can take place at several stages in an evaporation cascade. Therefore, the fission cross section should with increasing energy approach a value σ_{lim} that corresponds to the total interaction cross section for reactions which deposit an excitation energy that is higher than the fission threshold E_f for the nuclei in question. With U^{238} as the target, this energy is around 5 MeV and its fission excitation functions have been used to define our σ_R values.³ With this target, fragment-fragment angular-correlation studies have shown fission from both CF and ICF reactions. The ICF reactions are dominated by reactions involving the net transfer of approximately four nucleons—which have the same velocity as the ions—to the target nucleus.¹²

With O^{16} and C^{12} incident on Bi and lighter targets, the ICF reactions contribute at most 1% to the total fission cross section.⁸ Here four-nucleon transfer yields nuclei with E_B around 20 MeV or higher, and the excitation energy is not high enough to give an appreciable fission cross section.² With Ne^{20} incident on Au and Bi, the ICF reactions contribute 7 and 10%, respectively.⁸ For these systems in a region where first-chance fission is dominating, the experimental value for Γ_f/Γ_n will then be given by

$$\Gamma_f/\Gamma_n = (1 + \Gamma_{CP}/\Gamma_n) / (\sigma_{CF}/\sigma_f - 1). \quad (4)$$

Here Γ_{CP} is the level width for charged-particle evaporation. To evaluate Γ_f/Γ_n we therefore also have to know the values for the ratios σ_{CF}/σ_R and Γ_{CP}/Γ_n .

Information about σ_{CF}/σ_R can be obtained from:

(1) Fission-excitation functions for targets light enough that only CF reactions will contribute to fission but heavy enough that all the nuclei formed in these reactions will fission. Then σ_f should approach σ_{CF} as E increases.

(2) Fragment-fragment angular-correlation studies of targets as heavy as U^{238} . Here both CF and ICF reactions produce nuclei that eventually will undergo fission; at maximum ion energy the difference in linear momenta of the nuclei from the two processes is large enough to give fragment-fragment correlation functions that can be easily separated.^{7,10}

(3) Measurements of $f_n = (\sum \sigma_{xn})/\sigma_R$ for lighter targets when fission and charged-particle evaporation can be ignored. Here σ_{xn} is the cross section for a product in a (HI, xn) reaction. These reactions have been shown to proceed via a CF process and therefore we have $f_n = \sigma_{CF}/\sigma_R$.

It appears that σ_f/σ_R is a function of the ion used

and the ions therefore have to be considered separately.

Britt and Quinton⁵ obtained the values 0.63 and 0.61 for σ_f/σ_R for $Au + C^{12}$ and $Bi + C^{12}$, respectively, independent of E . Goldberg, Reynolds, and Kerlee⁷ reported the same quantity to be 0.73 for $Au + 124\text{-MeV } C^{12}$, and 0.69 for $Pb^{208} + 124\text{-MeV } C^{12}$. Correlation studies¹² for $U^{238} + 124\text{-MeV } C^{12}$ gave $\sigma_{CF}/\sigma_R = 0.75$ and Alexander and Siminoff¹⁶ found the value 0.85 for f_n at $E = 50$ MeV for the system $Nd^{144} + C^{12}$.

With O^{16} the values from different sources are less conflicting. We see from Table I that for $Bi + O^{16}$ the σ_f/σ_R is 0.72, independent of E . For the system $Au + O^{16}$ σ_f/σ_R is 0.70 from $E = 100$ MeV up to maximum energy, and for $W + O^{16}$ σ_f/σ_R is 0.70 at the highest energies. Britt and Quinton obtained for the same quantity 0.79 for $Au + O^{16}$ and 0.72 for $Bi + O^{16}$ over a wide range of energies,⁵ and Goldberg *et al.*⁷ obtained 0.75 for $Pb^{208} + 166\text{-MeV } O^{16}$. Correlation measurements¹² for $U^{238} + 166\text{-MeV } O^{16}$ gave 0.70 for σ_{CF}/σ_R . Finally, Alexander and Siminoff determined f_n to be 0.70 for $Ce^{140} + O^{16}$ at an excitation of 75 MeV.

The data for Ne ions are not as complete as for O^{16} . For $Tb + Ne^{22}$ (see Table I), σ_f/σ_R is 0.45 from $E = 130$ MeV up to maximum energy. Here we then set $\sigma_f \approx \sigma_{CF}$ and hence $\sigma_{CF}/\sigma_R = 0.45$. Goldberg *et al.* obtained the values 0.64 and 0.75 for σ_f/σ_R for $Bi + 208\text{-MeV } Ne^{20}$ and $Pb^{208} + 208\text{-MeV } Ne^{20}$, respectively,⁷ which, corrected for contribution of ICF reactions to fission, correspond to σ_{CF}/σ_R values of 0.54 and 0.65. This is to be compared to 0.58 for the ratio σ_{CF}/σ_R deduced from correlation studies¹² of $U^{238} + 208\text{-MeV } Ne^{20}$ and to $f_n = 0.70$ for $Ba^{136} + Ne^{20}$ at $E = 75$ MeV.¹⁶

We will conclude from this that σ_{CF}/σ_R is nearly independent of target and excitation energy and has the value 0.72 ± 0.10 , 0.72 ± 0.03 , and 0.60 ± 0.10 for C^{12} , O^{16} , and Ne^{22} , respectively. These values will be adopted in the analysis.

Values of Γ_{CP}/Γ_n in heavy ion induced reactions might be deduced from cross sections σ_p and σ_α for evaporated p 's and α 's.

Britt and Quinton have measured σ_α in C^{12} and O^{16} induced reactions in Au and Bi.¹⁷ They found $\sigma_\alpha/\sigma_R = 0.1$ at 130 MeV of excitation and that this ratio decreased rapidly with decreasing excitation energy to 0.01 at 50 MeV. Using 147-MeV N^{14} , Watson found $(\sigma_p + \sigma_\alpha)/\sigma_R$ to be a strong function of the Z of the target.¹⁸ If we interpolate his curves, we find the ratio is about 0.1 for $Z_T = 80$, and 0.9 for $Z_T = 60$. His measurements of direct interaction α 's and p 's, however, show practically no variation with Z_T , in accordance with the above conclusions. For the system $Ni + 164\text{-MeV } O^{16}$, Knox *et al.* at 10.4 MeV/nucleon obtained $\sigma_\alpha/\sigma_R = 1.3$ and $\sigma_p/\sigma_R = 1.0$.¹⁹ The increased cross

¹⁶ J. M. Alexander and G. N. Simonoff, Lawrence Radiation Laboratory Report UCRL-10541, January 1963 (unpublished).

¹⁷ H. C. Britt and A. R. Quinton, Phys. Rev. **124**, 877 (1961).

¹⁸ J. C. Watson, Yale University (private communication).

¹⁹ W. J. Knox, A. R. Quinton, and C. E. Anderson, Phys. Rev. **120**, 2120 (1960).

section for charged particle evaporation with decreasing Z of the target can be attributed to decrease in the barrier for α 's and p 's and to a decrease in fission competition as the Z of the CF nucleus is decreased.

The effect of charged-particle evaporation can be seen in the fission-excitation functions for targets lighter than W . For instance (as is seen from Table I) in the O^{16} bombardments, the maximum value of σ_f/σ_R decreases rapidly as the Z of the target decreases. We find it unreasonable to attribute this to a sudden fast decrease in σ_{CF}/σ_R . Rather this is mainly a result of the increased competition from charged-particle evaporation. Adding Watson's values for $(\sigma_p + \sigma_\alpha)^{18}$ to σ_f yields values that are at least 0.70 σ_R . Evaporation of an alpha particle will reduce E by 25 MeV¹⁸; this will greatly reduce the chance for a second-chance fission in a reaction with a light target. Other effects may also play a role as will be discussed under Sec. IV D.

Alexander and Siminoff¹⁶ found f_n to decrease slowly with E for $Z_T \approx 60$ ($df_n/dE \approx -5 \times 10^{-3}$ MeV⁻¹); this decrease can be attributed to an increased competition from charged-particle evaporation. In that case, $\sigma_{CF}/\sum \sigma_{xn}$ —and thus Γ_{CF}/Γ_n —will be around 0.4 at $E = 110$ MeV.

The conclusion we reach from these rather incomplete data is that at moderate energies we have $\Gamma_{CF}/\Gamma_n \ll 1$. We will therefore ignore this quantity in formula (4). This might introduce an error of as much as 40% in Γ_f/Γ_n at say 110 MeV for the lighter targets. However, an error of that order of magnitude will not significantly alter the results of the analysis shown in Sec. IVB. The experimental Γ_f/Γ_n values are therefore given by

$$\Gamma_f/\Gamma_n = 1/(\sigma_{CF}/\sigma_f - 1). \quad (5)$$

Curves for Γ_f/Γ_n for the different systems calculated according to Eq. (5), using the above accepted values for σ_{CF}/σ_R , are given in Figs. 3 and 4.

B. Comparison of Experimental Γ_f/Γ_n with Theoretical Values

There are several formulas based on statistical models that relate the ratio Γ_f/Γ_n to other quantities. The best fit to experimental data is obtained with the level-density expression $(E) = \text{const} \times \exp[2(aE)^{1/2}]$ where a is the level-density parameter. For systems with no rotation, the ratio is given by¹

$$\frac{\Gamma_f}{\Gamma_n} = \frac{K_0 a_n (E - E_f)}{4A^{2/3} a_f [2a_n^{1/2} (E - B_n)^{1/2} - 1]} \times \exp\{2a_f^{1/2} (E - E_f)^{1/2} - 2a_n^{1/2} (E - B_n)^{1/2}\}. \quad (6)$$

Here A is the mass number of the compound nucleus, E is its excitation energy in excess of the ground state, $K_0 \approx 9.8$ MeV, a_n and a_f are the level-density parameters for neutron evaporation and fission, respectively, B_n is the neutron-binding energy that can be taken

from Cameron's tables,¹⁵ and E_f is the experimental-fission threshold for a nonrotating nucleus.

The quantity E_f is equal to $m_s^0 - m_e^0$ where m_e^0 and m_s^0 are its masses at saddle and equilibrium (ground-state) configurations, respectively.

As is demonstrated in Fig. 4, Γ_f/Γ_n is not only a function of E . Here we see that by changing the mass of the ion, and thus the angular momentum of the compound nucleus, the ratio Γ_f/Γ_n is altered. Classically, rotational energy is associated with the angular momentum. It is argued that the level density is not initiated before the excitation energy exceeds the rotational energy.¹ Rotation will also change the shapes of the nuclei at the two configurations and thus their masses and moments of inertia. The level density at an angular momentum l will then be initiated at an energy

$$\text{for fission} \quad R_s^l + m_s^l - m_e^0,$$

and

$$\text{for neutron} \quad R_e^l + m_e^l - m_e^0 + B_n,$$

where R_s^l and R_e^l are the rotational energies at saddle and equilibrium, and m_s^l and m_e^l are the corresponding masses at these configurations. These parameters are functions of l .

There are liquid-drop model calculations of m_s^l and m_e^l .^{20,21} However, both R_s^l and R_e^l are complex functions of l . It was therefore felt unrealistic to attempt to tie the analysis in with the liquid-drop model at this stage. Instead, we attempt to simplify the situation somewhat by postulating that the changes in masses are directly correlated to changes in rotational energies. We can then set

$$m_e^l - m_e^0 = R_e^0 - R_e^l \quad (7)$$

and

$$m_s^l - m_s^0 = R_s^0 - R_s^l, \quad (8)$$

where R_e^0 and R_s^0 are the rotational energies at equilibrium and saddle when there are no changes in shapes with l . The level densities are therefore initiated at the energies

$$\text{for fission} \quad E_f + R_s^0$$

and

$$\text{for neutron} \quad B_n + R_e^0.$$

The rotational energy at equilibrium is given by

$$R_e^0 = \hbar^2 I_n^2 / 2\mathcal{I}_e^0, \quad (9)$$

where I_n is the angular momentum of the nucleus after the emission of one neutron, and \mathcal{I}_e^0 is the effective moment of inertia at the equilibrium configuration for an undistorted (spherical) nucleus. The quantity I_n is approximately equal to the angular momentum I of the compound nucleus that again is equal to the angular momentum l_{CF} brought in by the ion in a CF reaction.

²⁰ G. A. Pik-Pichak, Zh. Eksperim. i Teor. Fiz. **34**, 341 (1958) [English transl.: Soviet Phys.—JETP **7**, 238 (1958)].

²¹ J. R. Hiskes, thesis, Lawrence Radiation Laboratory Report UCLR-9275, June 1960 (unpublished).

The rotational energy at saddle is given by²²

$$R_s^0 = \hbar^2 I^2 / 2\mathfrak{F}_1 + \hbar^2 K^2 / 2\mathfrak{F}_{\text{eff}},$$

where

$$1/\mathfrak{F}_{\text{eff}} = 1/\mathfrak{F}_{\perp} - 1/\mathfrak{F}_{\parallel}. \quad (10)$$

Here \mathfrak{F}_{\perp} and \mathfrak{F}_{\parallel} are the moments of inertia about an axis perpendicular and parallel to the nuclear axis, respectively. The quantity K is the projection of I on the same axis.

We use the approximation that the average value $\langle \Gamma_f / \Gamma_n \rangle$, which we are measuring, is obtained at the average values of the rotational energies. The mean square (ms) of K is K_0^2 , which is given by

$$K_0^2 = T\mathfrak{F}_{\text{eff}} / \hbar^2, \quad (11)$$

where T is the nuclear temperature. The nuclear temperature is expected to vary linearly with $[(E - E_f - R_s^0) / a_f]^{1/2}$ and thus approximately linearly with I^2 for a particular ion. The average values of the rotational energies are then given by

$$\langle R_s^0 \rangle = \hbar^2 \langle l_{\text{CF}}^2 \rangle / 2\mathfrak{F}_e^0 \quad (12)$$

and

$$\langle R_s^0 \rangle = \hbar^2 \langle l_{\text{CF}}^2 \rangle / 2\mathfrak{F}_{\perp}^0 + T/2 \equiv \hbar^2 \langle l_{\text{CF}}^2 \rangle / 2\mathfrak{F}_s^0. \quad (13)$$

The ICF reactions are shown¹² to take place for the highest l waves of the incoming ion and thus to a good approximation

$$\langle l_{\text{CF}}^2 \rangle = \langle l_R^2 \rangle / (1 + \sigma_{\text{ICF}} / \sigma_{\text{CF}}),$$

where

$$\langle l_R^2 \rangle \approx (9/4) \langle \bar{l}_R \rangle^2. \quad (14)$$

Here $\langle l_R^2 \rangle$ is the ms value and \bar{l}_R is the average value of the angular momentum in a total interaction as obtained from cross-section calculations. The final expression for the ratio¹ will then be

$$\frac{\Gamma_f}{\Gamma_n} = \frac{K_0 a_n [2a_f^{1/2} (E - E_f - R_s^0)^{1/2} - 1]}{4A^{2/3} a_f (E - B_n - R_e^0)} \times \exp\{2a_f^{1/2} (E - E_f - R_s^0)^{1/2} - 2a_n^{1/2} (E - B_n - R_e^0)^{1/2}\}. \quad (15)$$

In our analysis we neglect the effect of the quantum-mechanical penetrability of the fission barrier on Γ_f , since E in our cases is much larger than E_f . This effect has been considered by Burnett *et al.* in their analysis of $\text{Au}(\alpha, f)$ at E around E_f .²³

It is now possible, by some suitable choice of the parameters E_f , a_n , a_f , \mathfrak{F}_e^0 , and \mathfrak{F}_s^0 , to fit values calculated in accordance with formula (15)²⁴ to the experi-

²² I. Halpern and V. Strutinski, in *Proceedings of the Second International Conference on Peaceful Uses of Atomic Energy, Geneva, 1958* (United Nations, New York, 1958), Vol. 15, p. 408.
²³ D. S. Burnett, R. C. Gatti, F. Plasil, P. B. Price, W. J. Swiatecki, and S. G. Thompson, Lawrence Radiation Laboratory Report UCRL-11079, November 1963 (unpublished).

²⁴ J. E. Clarkson, Lawrence Radiation Laboratory, August 1961 (private communication).

TABLE II. Various parameters used in calculations of Γ_f / Γ_n when $a_n = 20 \text{ MeV}^{-1}$, $\mathfrak{F}_e = \frac{2}{3}\mathfrak{F}_s = \mathfrak{F}_{\text{rig}}$, and a comparison with liquid-drop-model values for the fission barrier.

System	Compound nucleus	$\hbar^2 / \mathfrak{F}_{\text{rig}}^a$ (keV)	a_f / a_n	E_f (MeV)	$E_{f_{\text{exp}}}^L$ (MeV)	E_f^L (MeV)
Cs+O ¹⁶	Eu ¹⁴⁹	8.43	1.22	32.5	32.8	37.0
Pr+O ¹⁶	Ho ¹⁶⁷	7.72	1.15	26.5	27.9	30.3
Tb+O ¹⁶	Ta ¹⁷⁵	6.45	1.19	25.1	24.1	24.5
Tm+C ¹²	Re ¹⁸¹	5.82	1.20	24.0	22.9	22.2
Ho+O ¹⁶	Re ¹⁸¹	5.82	1.21	23.9	22.8	22.2
Tb+Ne ²²	Re ¹⁸¹	5.82	1.25	24.3	23.2	22.2
Er ¹⁷⁰ +O ¹⁶	Os ¹⁸⁶	6.09	1.23	24.2	23.2	22.7
Tm+O ¹⁶	Ir ¹⁸⁵	5.62	1.19	20.4	19.0	18.1
Yb ¹⁷⁴ +O ¹⁶	Pt ¹⁹⁰	5.87	1.19	19.8	18.2	18.5
Lu+O ¹⁶	Au ¹⁹¹	5.57	1.20	18.4	16.3	15.5
W ¹⁸² +O ¹⁶	Po ¹⁹⁸	5.25	1.25	17.0	15.6	9.7
Au+He ⁴	Tl ²⁰¹		1.33 ^c	22.5 ^c	18.2 ^c	16.2
Au+He ⁴	Tl ²⁰¹		1.19 ^b	19.5 ^b	15.2	16.2
Tl ^{208,209} +He ⁴	Bi ^{207,209}		1.24 ^b	18.8 ^b	12.2	14.2
Pb ²⁰⁶ +He ⁴	Po ²¹⁰		1.28 ^b	18.0 ^b	10.2	12.0
Bi+He ⁴	At ²¹³		1.33 ^b	14.9 ^b	10.5	10.5

^a $\mathfrak{F}_{\text{rig}}$ is the rigid-body moment of inertia for a spherical nucleus.

^b Data taken from Huizenga *et al.* (Ref. 2).

^c Data taken from Burnett *et al.* (Ref. 23).

mental values estimated from formula (5). It turned out, however, that all of them could not be uniquely determined. In particular, the level-density parameters and the moments of inertia could take on a wide range of values. We therefore had to choose "best" values for a_n , \mathfrak{F}_e^0 , and \mathfrak{F}_s^0 and the ratio a_f / a_n and E_f were to be determined from the analysis.

The choice of a_n is not very important as has been pointed out by Huizenga *et al.*² We used the value 20 MeV^{-1} since this has also been considered by Huizenga *et al.* and thus we can directly compare their results with ours.

The quantity \mathfrak{F}_e^0 is expected to be of the order of $\mathfrak{F}_{\text{rig}}$ at high excitation energies. Here $\mathfrak{F}_{\text{rig}}$ is the rigid-body moment of inertia for a spherical nucleus and is given by

$$\mathfrak{F}_{\text{rig}} = \frac{2}{5} r_0^2 A^{5/3}, \quad \text{where } r_0 = 1.22 \times 10^{-13} \text{ cm.}$$

With $\mathfrak{F}_e^0 = \mathfrak{F}_{\text{rig}}$ we obtain from Eq. (13) the ratio $\mathfrak{F}_e^0 / \mathfrak{F}_s^0$ to be around 0.5. The ratios a_f / a_n and $\mathfrak{F}_e^0 / \mathfrak{F}_s^0$ were assumed to be independent of E . The validity of these assumptions is discussed in Sec. IV D.

Values for $\hbar^2 / 2\mathfrak{F}_{\text{rig}}$, a_f / a_n , and E_f for the different systems with $a_n = 20$, $\mathfrak{F}_e^0 / \mathfrak{F}_{\text{rig}} = 1$, and $\mathfrak{F}_e^0 / \mathfrak{F}_s^0 = 0.5$, are given in Table II. We have also included values from Huizenga *et al.*² which were obtained in a similar analysis.

The fit to the experimental Γ_f / Γ_n curves are shown in Figs. 3 and 4. With the exception of the systems Tm+C¹² and Cs+O¹⁶, we see an excellent fit over the entire steep part of the curves that in many cases is of the order of 25 MeV. A possible explanation for the poorer fit for these two systems is given in Sec. IV D. The systems Bi+O¹⁶ and Au+O¹⁶ could, of course, not be analyzed.

Values for the parameters a_f/a_n and E_f do not change appreciably with the absolute values of Γ_f/Γ_n . For example, we analyzed the data for the case $\sigma_{CF}/\sigma_R=1$ that corresponds to a decrease in Γ_f/Γ_n by 30, 30, and 40% for C^{12} , O^{16} , and Ne^{22} , respectively. This changed E_f by less than 1 MeV with a_f/a_n unchanged. Similarly a_f/a_n , and especially E_f , are fairly independent of our choice of \mathfrak{F}_e^0 and \mathfrak{F}_e^0 . For instance, we analyzed the system $Pr+O^{16}$ with $\mathfrak{F}_e^0/\mathfrak{F}_{rig}$ in the range 0.5 to 1.0 and $\mathfrak{F}_e^0/\mathfrak{F}_s^0$ from 0.5 to 1.0 and found a_f/a_n and E_f to vary only by 4 and 2%, respectively.

The slope of Γ_f/Γ_n is important for both a_f/a_n and E_f ; as is seen from Fig. 3 the lighter the target the shorter and more uncertain the steep part is. Therefore, the uncertainty in both a_f/a_n and E_f increases with decreasing mass of the target.

A possible decrease in σ_{CF}/σ_R or an increase in Γ_{CF}/Γ_n with E will make the slope of Γ_f/Γ_n steeper. An order of magnitude estimate of these effects is obtained from the measurements of f_n . Alexander and Siminoff's value $df_n/dE \approx 5 \times 10^{-3} \text{ MeV}^{-1}$ corresponds to an increase in $d(\Gamma_f/\Gamma_n)/dE$ of 0.007 MeV^{-1} over the value obtained when $\sigma_{CF}/\sigma_R = \text{constant}$. This increase will introduce an insignificant increase in a_f/a_n and E_f .

Considering all these effects, we set the uncertainties in a_f/a_n to increase from 5% for the heaviest to 7% for the lightest; in E_f the uncertainties increase from 2 MeV for the heaviest targets to 4 MeV for the lightest.

As is seen from Table II, E_f is increasing with decreasing mass of the targets. This variation is discussed separately in Sec. IV C.

The quantity a_f/a_n , however, is within the uncertainty of the analysis independent of nuclear type. (The slightly higher values of a_f/a_n in the closed-shell region might be entirely due to a possible decrease in the ratio with E as will be discussed under Sec. IV D.) This result is somewhat surprising since one would expect a_n to approach a_f as we go away from the closed shell. This therefore indicates that the same fundamental difference persists: The shell structure at saddle is completely destroyed, whereas at equilibrium the shells are still effective outside the closed-shell region. The average value of a_f/a_n from Table II is 1.22 with a standard deviation of 0.05.

C. The Fission Barrier

It is especially gratifying that the values for E_f are fairly independent of the choice of the other parameters. We believe therefore that these values can be taken seriously. In the following, an attempt is made to compare them to those E_f^L predicted by the liquid-drop model. First, E_f has to be corrected for shell and pairing effects to yield an "experimental" liquid-drop-barrier value $E_{f \text{ exp}}^L$:

$$E_{f \text{ exp}}^L = E_f + \Delta_s^c + \Delta_p^c - \Delta_s^f - \Delta_p^f = E_f + \Delta_f, \quad (16)$$

where Δ_s^c and Δ_p^c are the shell and pairing corrections

for the ground-state mass of the compound nucleus, and Δ_s^f and Δ_p^f are the corresponding corrections of the saddle. As argued above, the nucleus is so distorted at saddle that the shell structure is destroyed and thus we have $\Delta_s^f=0$. We further use the approximation that the pairing energies are the same at the two configurations and therefore obtain $\Delta_f = \Delta_s^c$. Taking Cameron's reference mass as that of the liquid drop, values for Δ_s^c can be taken from his compilations.¹⁵ The resulting $E_{f \text{ exp}}^L$ values are given in Table II together with those from Huizenga *et al.*²

According to Cohen and Swiatecki²⁵ the barrier E_f^L for a charged liquid drop without rotation is in the region $\frac{1}{3} < x < \frac{2}{3}$ to a good approximation given by

$$E_f^L = 0.38(0.75 - x)E_s^0, \quad (17)$$

where $E_s^0 = 17.8A^{2/3}$ is the surface energy of a spherical liquid drop and $x = (Z^2/A)/(Z^2/A)_{\text{crit}}$. With the commonly used value 50.13 for $(Z^2/A)_{\text{crit}}$, we obtain values for E_f^L that are higher than $E_{f \text{ exp}}^L$. Instead, we obtain a good fit with the value $(Z^2/A)_{\text{crit}} = 48.0$. The corresponding E_f^L values are given in the last column of Table II. As is seen, $E_{f \text{ exp}}^L$ has a standard deviation of around 2 MeV from E_f^L . Huizenga *et al.* quote the same error in their analysis.² There appears to be no systematic deviation of $E_{f \text{ exp}}^L$ from E_f^L in and outside the region of the closed shell. We might conclude from this that no shell and pairing-energy-correction term Δ_n should be introduced in the level-density formula for neutron emission as was considered by Huizenga *et al.* Introduction of such a term makes E_f higher in the closed-shell region. The values of E_f taken from Huizenga *et al.* are from the analysis in which $\Delta_n=0$ and $a_n=20$. We have also included values from Burnett *et al.* for the system $Au(\alpha, f)$.²³

By taking into account systematic errors, we suggest the value 48.0 ± 1.0 for $(Z^2/A)_{\text{crit}}$ for the nuclei considered in this investigation. It must be pointed out that with this value we obtain reasonable values for E_f in the uranium region using the liquid-drop-model formula²⁵ $E_f^L = 0.83(1-x)^3 E_s^0$. However, for still heavier nuclei the calculated values are too low when $(Z^2/A)_{\text{crit}} = 48.0$ is used.

D. The Γ_f/Γ_n Functions at Higher Energies

We notice that the calculated Γ_f/Γ_n values are higher than the experimental ones at energies above the steep part of the curve. The deviation increases with increasing excitation energy. After considering several chance fissions we see that the relation should in fact be reversed.

This discrepancy can be removed if (a) Γ_{CF} increases with E , (b) σ_{CF}/σ_R decreases with E , (c) $\mathfrak{F}_e^0/\mathfrak{F}_s^0$ increases with E , and (d) a_f/a_n decreases with E . The factors (a) and (b) have been shown above to be

²⁵ S. Cohen and W. J. Swiatecki, *Ann. Phys. (N. Y.)* **22**, 406 (1963).

contributing, but it is felt that they are not large enough to account for the total difference.

The possible variation of $\mathcal{F}_e^0/\mathcal{F}_s^0$ and a_f/a_n with E can at best be discussed qualitatively. Examining Eq. (13), we see that \mathcal{F}_e^0 is likely to increase with increasing E . As to the variation of \mathcal{F}_e^0 with E , the shell and the liquid-drop models do not even agree qualitatively. The shell model predicts \mathcal{F}_e^0 to increase with E as shells are destroyed and the number of nucleons sharing the angular momentum are increasing. According to the liquid-drop model, \mathcal{F}_e^0 decreases with E as a result of a decrease in the viscosity of the drop with temperature. For both models, \mathcal{F}_{rig} is the maximum value for \mathcal{F}_e^0 . In the compound nucleus picture the nucleons interact strongly and are thus sharing the angular momentum. Here then $\mathcal{F}_e^0 \approx \mathcal{F}_{\text{rig}}$ independent of E .

The quantity a_n is expected to approach a_f as E increases as a result of an onset of a destruction of the shells at equilibrium configuration. The ratio a_f/a_n , accordingly, should decrease with E .

The variation of $\mathcal{F}_e^0/\mathcal{F}_s^0$ or a_f/a_n with E does not have to be drastic. For instance, at 104 MeV of excitation for the system $\text{Pr}+\text{O}^{16}$, we obtain agreement between estimated and experimental Γ_f/Γ_n values with either $\mathcal{F}_e^0/\mathcal{F}_s^0=0.54$ or $a_f/a_n=1.13$ instead of the values 0.5 and 1.15 used at lower energies.

We may therefore conclude that the discrepancy at higher energies can be accounted for. These effects also explain the poorer fit for the systems $\text{Tm}+\text{C}^{12}$ and $\text{Cs}+\text{O}^{16}$ which have more shallow curves than the other systems. This does not, however, significantly alter the values for E_f obtained in our analysis.

V. CONCLUSIONS

There are some aspects of this investigation that should be commented upon. The first is related to the observation that $\sigma_{\text{CF}}/\sigma_R$ appears to be independent of the excitation energy; instead, $\sigma_{\text{CF}}/\sigma_R$ is a function of the ion used. A knowledge of this value is, as we have seen, not critical for our analysis. However, it is important for other studies of the decay of CF nuclei where an estimation of angular momenta is imperative. The data available on $\sigma_{\text{CF}}/\sigma_R$ are conflicting and incomplete and it might therefore be worthwhile to carefully measure this quantity for various systems. As we pointed out, this can be done by measuring σ_f as a function of E in the interaction of various heavy ions with targets that are light enough that "grazing" reactions will not lead to fission and heavy enough that nuclei produced in a CF reaction will eventually decay

by fission. It is also evident that more data on σ_p and σ_α are needed both as functions of Z_T and especially E .

The second comment has to do with the effect of rotation on the level width for fission. As mentioned, rotation might change the shapes and thus the moments of inertia and masses of the equilibrium and the saddle configurations. This introduces so many parameters in the theoretical Γ_f/Γ_n formulas that the analysis becomes meaningless. The data can therefore not be used to find experimental values for fission barriers or moments of inertia for a rotating nucleus.

The analysis has been made possible by the introduction of the postulate that at either of the two configurations any change in mass due to rotation is equal to the difference between the rotational energy of the nucleus with and without change in shape. The analysis then yields values for the experimental fission barrier of a nonrotating nucleus. Values for the rotating case might be obtained from fragment-angular distributions.

The fission barriers corrected for shell effects fit well the liquid-drop-model formula, and this model therefore appears to be successful in explaining the gross features of the fission process in the lighter and medium heavy region of the periodic table.

Our concluding remark concerns the level-density parameters. Absolute values for these quantities cannot be obtained from the fission-excitation functions. However, from the analysis, we note that the ratio a_f/a_n is larger than one and is nearly independent of nuclear type, reflecting the destruction of the shells at saddle and the preservation of a degree of bunching of the levels²⁶ at the equilibrium configuration even outside the closed-shell region.

ACKNOWLEDGMENTS

The author is most of all indebted to Victor E. Viola, Jr., for his active participation in the early phases of this work before leaving for CERN. He thanks Jack E. Clarkson for allowing him to use his tables for the Γ_f/Γ_n functions, Wladyslaw J. Swiatecki for helpful discussion, and Albert Ghiorso for his interest in and support of this work. He would also like to thank Mrs. Roberta B. Garrett for the valuable aid in processing the data, Robert M. Latimer and Walter F. Stockton for the silicon detectors, William W. Goldsworthy and Almon E. Larsh for help with the electronics, and Daniel O'Connell for the targets. The HILAC crew is acknowledged for excellent beams.

²⁶ W. J. Swiatecki, Lawrence Radiation Laboratory (private communication).